

# Nuclear Magnetic Resonance Spectroscopy of Frozen Phosphatidylcholine–D<sub>2</sub>O Suspensions: A New Technique for measuring Hydration Forces

Zhenjie Yan, James Pope and Joe Wolfe\*

School of Physics, The University of New South Wales, Kensington, Australia

At temperatures below freezing, lamellar phases of lipids in water separate into regions of ice in equilibrium with regions of lamellar phase with reduced water content. The repulsive force per unit area between lamellae is the negative of the pressure in the unfrozen, interlamellar water, which is determined by the chemical potential and thus by the temperature. When deuteriated water is used, the fraction remaining unfrozen is determined from its contribution to the nuclear magnetic resonance signal. When the molecular area in the plane of the lamellae and the density of water are known or may be inferred, the interlamellar separation may be calculated. We report the use of this technique to measure force–hydration and force–distance curves at freezing temperatures for egg yolk lecithin.

When surfaces separated by water are brought to separations of about a nanometre, the force between the surfaces is dominated by a large repulsion. This force decreases approximately exponentially with separation with a characteristic distance of *ca.* 0.2 nm. It is usually called the hydration force, and some researchers attribute it to the non-random orientation of water molecules within a few molecular layers of the surface.<sup>1,2</sup> Another group attributes it to a combination of modes of thermal motion of the surface.<sup>3</sup>

These large short-range forces are of considerable importance in cryobiology.<sup>4</sup> When biological tissues or cell suspensions are frozen, the extracellular solution freezes first. The extracellular solutes are concentrated in the remaining unfrozen water and, except at very high freezing rates, the cell is dehydrated osmotically. As the temperature falls to  $-10$  or  $-20$  °C, the water content of the cell falls to a small fraction (typically several per cent), and all the non-aqueous components are forced closely together and their separation enters the range in which hydration forces dominate. This produces large anisotropic stresses in the membranes and it has been proposed that this may be responsible for the freezing damage characterised by loss of osmotic response in cells and tissues frozen in this range.<sup>5,6</sup> This hypothesis invites measurements of inter-membrane forces at freezing temperatures.

In 1976 LeNeveu *et al.* reported measurements of forces between the membranes of lipid–water lamellar phases using the osmotic stress technique.<sup>7</sup> In 1977 Israelachvili reported measurement of the force between molecularly smooth mica surfaces in aqueous solution using the surface forces apparatus.<sup>8</sup>

In the osmotic stress technique, the degree of hydration of the lamellar phase of lipid water mixtures is varied by controlling the chemical potential of the water. To reduce its chemical potential, water in the lamellar phase can be allowed to equilibrate with a bulk solution of known osmotic pressure, or with an atmosphere of known vapour pressure of water. (This atmosphere is produced by equilibration with a saturated salt solution.) The force per unit area between the membranes equals the suction in the interlamellar water, and that is determined from the chemical potential of the external water phase. The inter-membrane separation is then calculated from the results of X-ray diffraction measurements. This technique has been used to study a range of lipids.<sup>1,9,10</sup>

In the surface forces apparatus (SFA), the separation is determined by optical interferometry and the force is mea-

sured directly using the deflection of a calibrated spring. The SFA has also been used to measure forces between membranes which have been deposited on the mica surfaces.<sup>11–13</sup>

There are practical difficulties in using the two techniques mentioned above to make measurements of inter-membrane forces at freezing temperatures. In the SFA, ice in the bulk phase would prohibit force measurements. The osmotic stress technique would require considerable modification for use at freezing temperatures.

We report the freezing behaviour of lipid lamellar phases in deuteriated water and we describe a new technique for measuring forces in lipid–water phases at freezing temperatures. The temperature is used to control the chemical potential of water, and thus the inter-membrane pressure. The hydration of the lamellar phase is calculated from the unfrozen fraction of deuteriated water which is derived from the intensity of its characteristic signal in nuclear magnetic resonance (NMR). The inter-membrane separation may also be estimated. We report force–hydration and force–distance relations at freezing temperatures for lamellar phases of egg yolk lecithin, a model membrane system whose properties have been well studied at higher temperatures using a variety of techniques.

## Theory

The water in a lipid lamellar phase is confined to thin (*ca.* nm) layers between the hydrophilic surfaces of the two adjacent lipid bilayer membranes (Fig. 1). For temperatures above *ca.*  $-30$  °C, ice does not form in these thin layers. For suction less than about 100 MPa, the water in these thin layers does not cavitate. The Gibbs free energy of formation of a domain of ice or a domain of water vapour in liquid water includes both volumetric and surface terms. For a spherical domain with radius *r*, the free energies are respectively:

$$G_{\text{ice}} = \rho q_{\text{fus}} \left( \frac{T}{T_c} - 1 \right) \frac{4}{3} \pi r^3 + \gamma_{\text{iw}} 4\pi r^2$$

and

$$G_{\text{vap}} = P \frac{4}{3} \pi r^3 + \gamma_w 4\pi r^2$$

where  $\rho$  is the density of water,  $q_{\text{fus}}$  the latent heat of fusion,  $T_c$  the bulk melting temperature,  $P$  the pressure ( $< 0$ ) in the liquid phase,  $\gamma_w$  the free energy per unit area of the vapour/water interface and  $\gamma_{\text{iw}}$  that of the ice/water interface. In the

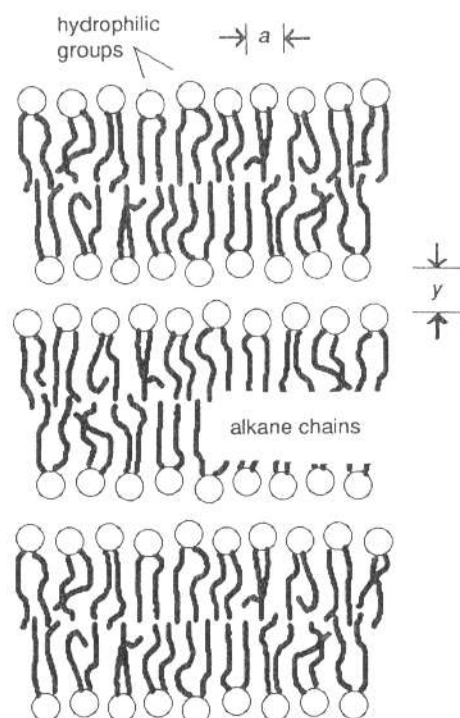


Fig. 1 Simple sketch showing parameters which are important to our analysis. Each lipid molecule occupies an area  $a$  in the plane of the lamellae. The separation between the density weighted interfaces is  $y$ .

absence of nuclei for freezing or for cavitation, the critical radii for ice formation and for cavitation are obtained by setting the above expressions to zero, whence:

$$r_{\text{ice}}^* = \frac{3\gamma_{\text{iw}}}{\rho q_{\text{fus}}(1 - T/T_c)}$$

and

$$r_{\text{cavitation}}^* = -\frac{3\gamma_w}{P}$$

First consider ice formation. At  $T = 260$  K, and using standard values, the critical radius for ice formation is *ca.* 6 nm. Thus spontaneous ice formation in the interlamellar spaces is unlikely. For this reason, supercooling of 10 K or more is possible in the water in lamellar phases, but may be avoided by cooling to low temperatures and then heating to the temperature of interest. When freezing does occur, the ice forms domains with dimensions much larger than 6 nm, in equilibrium with a reduced volume of unfrozen water between the lamellae (further discussed in the Results section).

Next consider cavitation. At a suction of 100 MPa, the critical radius for cavitation is *ca.* 2 nm. The formation of vapour domains between the lamellae is therefore unlikely, even though large suctions ( $P < 0$ ) may occur. The intermembrane repulsion within the lamellar phase is balanced by the (negative) hydrostatic pressure in the thin water layers. At low hydration (small separation), the hydration repulsion can be quite large: up to tens of MPa at distances of less than 1 nm. The suction in the aqueous region is equally large, but the hydrophilic surfaces and the small dimensions of the interlamellar water allow such large suctions without cavitation.

In a lamellar phase at 'full hydration', the interlamellar water is in equilibrium with bulk water, so its chemical potential equals that of water in the standard state. For a lamellar phase at less than full hydration, the chemical poten-

tial of the water is less than that of the standard state, *i.e.* work must be done to dehydrate the fully hydrated lamellar phase. In energy equations, this energy can be included in one of two different ways. One way is to define an energy of hydration which is itself a function of the degree of hydration. This convention is not adopted by those investigating hydration forces because it gives little further insight. In the system of accounting adopted here, the work done in removing water from the bilayer is treated as the work done in overcoming a repulsive force between the lamellae: hence the name hydration force. The equivalence of the two pictures is established by stating that, for a given area of interface, the hydration force equals the derivative of the hydration energy with respect to separation.

### Calculating the Pressure in the Water

Consider first the equilibrium between pure ice and pure water at  $T = T_c$ , the equilibrium bulk melting temperature. The enthalpy  $q_{\text{fus}}$  and entropy  $\Delta S$  of the transition are related by  $\Delta S = q_{\text{fus}}/T_c$ . To first order, we take  $\Delta S$  to be independent of temperature.

Now consider water (w) and ice (i) at equilibrium at  $T < T_c$ . The ice is in a macroscopic phase with  $P = 0$ , and the pressure  $P$  in the unfrozen water is negative at equilibrium.† For equilibrium:

$$\begin{aligned} \mu_i^0 &= \mu_w^0 + Pv_w = \mu_i^0 + q_{\text{fus}} - T\Delta S + Pv_w \\ &= \mu_i^0 + q_{\text{fus}} - T\frac{q_{\text{fus}}}{T_c} + Pv_w \end{aligned}$$

where  $\mu$  is the chemical potential, superscript 0 denotes the standard state,  $v_w$  is the volume of a unit quantity of water and  $P$  is the hydrostatic pressure in the interlamellar water. Rearrangement gives:

$$P = -\frac{q_{\text{fus}}}{v_w} \left(1 - \frac{T}{T_c}\right) \quad (1)$$

For  $\text{D}_2\text{O}$ , the density<sup>14</sup> is  $1105 \text{ kg m}^{-3}$ , the molar mass is  $0.020 \text{ kg mol}^{-1}$  and so its molecular volume,  $v_w$ , is  $3.01 \times 10^{-29} \text{ m}^3$ . Its melting temperature,  $T_c$ , is  $276.97 \text{ K}$  and its latent heat<sup>15</sup> is  $q_{\text{fus}} = 315 \text{ kJ kg}^{-1} = 2.61 \times 10^{-17} \text{ J molecule}^{-1}$ . Thus for  $\text{D}_2\text{O}$  eqn. (1) may be written  $P = (1.26 \text{ MPa K}^{-1})(T - T_c)$  where  $T_c = 276.97 \text{ K}$ . We are interested only in the range  $T < T_c$  where  $P$  is negative. We use the symbol  $F (= -P)$  for the force per unit area between the bilayers.

### Calculating the Separation

Let the sample contain  $n_1$  lipid molecules and  $n_w$  water molecules and let  $v$  be the number ratio  $n_w : n_1$ . At the bilayer water interface,  $a$  is the area per lipid in the plane of the interface and  $a_0$  its value at full hydration or zero imposed stress. The thickness of water between the volume-weighted interfaces is  $y$ . (See Fig. 1.)

The total volume of water before freezing is  $n_w v_w$ . We assume that the water is incompressible, which is a good approximation for pressures of magnitude much less than the

† In the alternative picture, the pressure of water in the lamellar phase is set at zero and one introduces instead the energy of hydration of the lipids. There is thus an extra energy term  $U(y)$  in the chemical potential for this energy of hydration. Equilibrium would be written thus:  $\mu_i^0 = \mu_w^0 + U(y)$ . In the 'pressure accounting' picture, the work done in removing water is the work  $P dv$  done in moving the surfaces closer together against their mutual repulsion. In the 'hydration accounting' picture the work done is work of hydration  $dU$  in removing water from the lamellar phase.

bulk modulus,<sup>14</sup> which is 2.0 GPa. The volume of unfrozen water in the lamellar phase at separation  $y$  is  $\frac{1}{2}n_1ay$ . This statement is a definition of the separation  $y$  as used here. The fraction  $f$  of unfrozen water is

$$f = \frac{n_1ya}{2} \frac{1}{n_w v_w} = \frac{ya}{2v_w}$$

so

$$a = 2 \frac{vf_w}{y} \quad (2)$$

As water is removed,  $y$  decreases. The area per molecule,  $a$ , also decreases. The extent of this contraction in the plane of the interface can be calculated using the area modulus  $k_a$  of the bilayer which is the ratio of lateral pressure  $\Pi$  to the area strain in the linear elastic limit:

$$\frac{a}{a_0} - 1 = -\frac{\Pi}{k_a} = \frac{Py}{k_a} \quad (3)$$

Higher order terms in the stress-strain relation will introduce errors in eqn. (3) for lateral pressures  $\Pi$  which are non-negligible compared with  $k_a$ . Kwok and Evans<sup>16</sup> give  $k_a = 140 \pm 16 \text{ mN m}^{-1}$  for egg yolk lecithin.  $\Pi$  is usually less than  $30 \text{ mN m}^{-1}$  in these experiments so the neglect of second-order terms should introduce an error of at most several per cent in area and thus in  $y$ . The area per molecule is also weakly dependent on temperature in the range that does not include the phase transition. This can be included using the coefficient  $\alpha$  of thermal expansivity in area, and the reference temperature  $T_r$  at which  $a_0$  is measured.

From the eqn. (2) and (3) for  $a$ , and including thermal expansion:

$$2 \frac{vf_w}{y} = a = a_0 \left[ 1 + \alpha(T - T_r) + \frac{Py}{k_a} \right]$$

which is quadratic in  $y$  and yields

$$y = -\frac{k_a}{2P} \left( 1 + \alpha(T - T_r) - \sqrt{\left\{ [1 + \alpha(T - T_r)]^2 + \frac{8vf_w P}{k_a a_0} \right\}} \right) \quad (4)$$

In the limit where  $\alpha = 0$  and to first order in  $Pv_w/k_a a_0$ , this gives  $y = 2vf_w/a_0$  which is the limit of eqn. (2) as  $a \rightarrow a_0$ .

## Materials and Methods

### Chemicals

D<sub>2</sub>O was purchased from Sigma (St. Louis, Mo). Its nominal purity was 99.9 at.% deuterium and it was used without further purification. Phosphatidylcholine from hen eggs (egg yolk lecithin, EYL) and dimyristoyl-phosphatidylcholine (DMPC) were purchased from Sigma. The DMPC was in the form of a powder and the EYL in 9:1 chloroform:methanol solution. The nominal purity was 99% and they were used without further purification. The EYL was batch V-EA which contained 0.1 wt.% butylated hydroxytoluenes in the solvent as anti-oxidant. (Force-distance relations are in principle affected by ionic impurities in the samples because ions screen the electric double-layer forces. In the region studied here, however, the short-range repulsion dominates and the force is almost totally independent of ionic concentration in the solution.<sup>9</sup>)

For each sample, a quantity of solution containing several tens of mg of lipid was added to a sample tube and dried under a stream of nitrogen gas until most of the chloroform evaporated. The tube was then placed in a desiccator also containing a quantity of P<sub>2</sub>O<sub>5</sub>, evacuated to ca. 0.1 Pa and

left for a minimum of 72 h to remove the remaining chloroform. The lipid was then a fine powder.

We took precautions to minimise the absorption of H<sub>2</sub>O by the sample. The desiccator was transferred to a dry-nitrogen atmosphere, and ca. 50 mg of dry lipid was transferred to an NMR sample tube with 5 mm diameter and 300  $\mu\text{m}$  wall thickness (Wilmad Glass, Buena, NJ). The thin walls were used to achieve large heat flux between the sample and the coolant. D<sub>2</sub>O of known volume was added from a microsyringe. The tube was temporarily sealed with Parafilm. The tube was then removed from the nitrogen atmosphere, the sample end was frozen in liquid nitrogen and the other end was immediately flame sealed. The sample was centrifuged several times and the tube was inverted between subsequent centrifugations.

### NMR

The NMR measurements were performed on a Bruker MSL-300 Spectrometer operating at 46.062 MHz. The probe was modified to provide extra thermal insulation and a larger coil was used to accommodate the sample temperature control plumbing. The coil was made from copper ribbon to improve the dissipation of heat generated by the radiofrequency pulses or conducted along the leads of the coil. Typically 1024 scans were summed at each temperature to achieve signal to noise ratios of between 20 and 100:1. The quadrupolar echo sequence was used.<sup>17</sup> The spectrum width was 10 kHz and the length of the 90° pulse was about 11  $\mu\text{s}$ .

### Temperature Control and Calibration

The difference signal between the set temperature and that of a thermocouple close to the sample was input to the differential feedback controller supplied with the spectrometer. This controlled the heating of a stream of pre-cooled air. The sample was centred in an insulating jacket and the stream of gas passed between the sample and the jacket, then passed over the thermocouple, then passed around the outside of the jacket, about which was wound the induction coil. Thus the cooling gas was also used to remove heat generated in the coil.

The temperature control was calibrated using a sample of pure D<sub>2</sub>O. When it is heated through the transition temperature, the strength of the narrow signal from the unfrozen component increases very rapidly with temperature. On the steep part of this curve, several runs were conducted with different values of flow in the cooling gas. At high rates, there was no detectable dependence on flow rate. Thus at these rates the cooling system is not limited by rate of heat removal, and so the sample has come into thermal equilibrium with the gas stream, whose temperature is then measured by the thermocouple. Similarly there was no dependence of this signal on the duty cycle of the radiofrequency pulses supplied to the coil. We therefore conclude that heat dissipation from the coil produced no change in the sample temperature.

A sample of pure D<sub>2</sub>O (180  $\mu\text{l}$ ) at the phase-transition temperature was also used to determine the heating and cooling times of the sample. Using such a sample, the set temperature was changed abruptly from 276 to 278 K. The signal intensity at first increased rapidly with time (as the ice melted) but there was no further increase in signal after 20 min. The heat flux required by this relatively large sample of D<sub>2</sub>O at its transition temperature was much greater than that required by any of the samples studied.

During the temperature runs, at least 20 min equilibration time was allowed between temperatures (discussed further in

the Results section). For all freezing experiments, the samples were cooled to  $-25^{\circ}\text{C}$  to initiate freezing (*i.e.* to avoid supercooling). Measurements were usually made in increasing order of temperature, with occasional returns to low temperature to ensure that there was no hysteresis.

### Calibration of Sensitivity

At any given temperature, the signal amplitude is assumed to be proportional to the number of contributing deuterons. The constant of proportionality is however a function of temperature because of the Curie law and because of the temperature dependence of the detecting circuit due to changes in resistance and in the  $Q$  of the coil. Deuterated methanol ( $\text{CH}_3\text{OD}$ ), which does not freeze over the temperature range, was used to calibrate the temperature dependence of the signal to the number of contributing deuterons. The sample of methanol had a deuteron content similar to that of the highly hydrated lipid samples.

### Calculation of the Water Signal

The peak in the spectrum which arises from unfrozen water has a width of typically 100 Hz. The width of the ice signal<sup>18</sup> is 240 kHz which is much larger than the scale used in these experiments. The two signals were separated by numerical differentiation of the spectrum. The narrow region including the differential of the peak was replaced by a linear interpolation. This function was then integrated and subtracted from the original spectrum to leave only the contribution to the spectrum from unfrozen water. This was integrated with respect to frequency to obtain what is hereafter referred to as the water signal. The water signal was then corrected for probe sensitivity as described above, and expressed as a fraction of its average value at temperatures above freezing.

### D-H Exchange?

We have no reason to expect deuterium exchange with hydrogens in the phosphatidylcholine headgroup. An upper bound for the exchange was determined thus: a spectrum was measured for a sample prepared as described above with 37 moles of  $\text{D}_2\text{O}$  per lipid and it remained sealed for 3 weeks. The sample was then unsealed and, to remove most of the  $\text{D}_2\text{O}$ , it was placed in a desiccator under vacuum in the presence of  $\text{P}_2\text{O}_5$  for 24 h. It was then rehydrated with  $\text{H}_2\text{O}$  and its spectrum was remeasured. After this treatment, the deuterium signal was undetectable, *i.e.* reduced by a factor of at least  $10^3$ . Thus less than 0.04 deuterons remain per lipid. This demonstrates that there is little exchange of deuterons with the hydrogens of the lipid. It also shows that there is very little water of hydration left after evacuation in the presence of  $\text{P}_2\text{O}_5$ .

## Results and Discussion

Fig. 2 shows the amplitude spectra of lamellar phases of EYL in  $\text{D}_2\text{O}$  at different temperatures over the range from  $-20$  to  $20^{\circ}\text{C}$ . All frequencies are measured with respect to the centre frequency of the deuterium resonance at 46.062 MHz. The peak with a linewidth of *ca.* 100–200 Hz indicates relatively freely rotating molecules and is attributed to unfrozen water between the lamellae. The width of the ice signal (240 kHz) is larger than the scale known here (10 kHz), so it forms the baseline. Beyer<sup>19</sup> showed that there is little exchange between the ice and water phase over the timescale of an NMR measurement.

The signal given by a pure sample of bulk  $\text{D}_2\text{O}$  water is a single Lorentzian line with linewidth of below 20 Hz. The

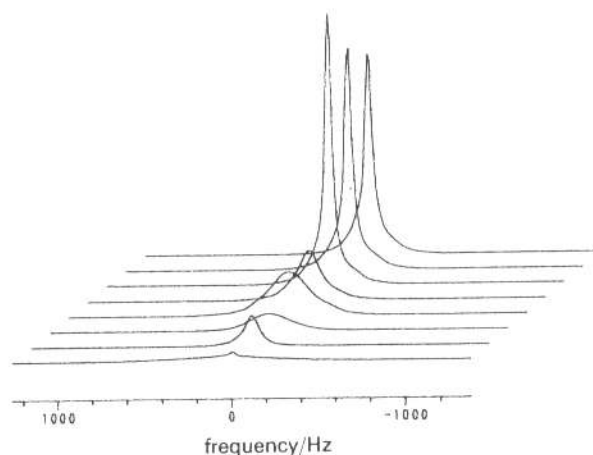


Fig. 2 Spectra of lamellar phases of EYL in  $\text{D}_2\text{O}$ , mole ratio 1 : 37. Starting with the lowest curve, the temperatures are  $-20$ ,  $-10$ ,  $0$ ,  $2$ ,  $4$ ,  $10$  and  $20^{\circ}\text{C}$ . Frequencies are measured with respect to the centre frequency of the deuterium resonance at 46.062 MHz (the 'zero' on the frequency scale). The ordinate is the Fourier transform of the potential difference across the induction coil and is in arbitrary units.

width of the water signals in Fig. 2 is larger than that of pure water because of the ordering near the lipid interface (a phenomenon extensively described previously<sup>20,21</sup>). At successively lower temperatures below freezing, the width of the signal first becomes larger. Over this range, the separation between lamellae is reduced, molecules of water spend on average more of their time close to the interface and so the average ordering of water molecules in the lamellar phase is increased. The spectrum at  $-10^{\circ}\text{C}$  shows a reduced ordering of water due to the proximity of the liquid crystal to gel transition.<sup>22</sup> At  $-20^{\circ}\text{C}$ , the signal shows a broad signal due to highly ordered lamellar water, and a narrow signal which we interpret as due to regions of supercooled water which has not equilibrated with the ice. We discuss this below.

### Fraction of Unfrozen Water

The total intensity of the water signal (the integral under the water peak in the Fourier transform) is the most important parameter in this study. For the temperatures above freezing, Fig. 2 shows that the area under the water peak decreases slowly with temperature. This is in part due to the inverse temperature dependence of the Curie law, and in part due to temperature-dependent sensitivity of the probe. This explicit temperature dependence was calibrated as described in Materials and Methods.

At temperatures below freezing ( $<4^{\circ}\text{C}$ ) the integral of the water signal decreases rapidly with decreasing temperature. Using the calibration described above, the unfrozen water content is calculated as a fraction of the water content above freezing. Samples were made with a range of mole ratios from 9 to 50 waters per lipid. The samples with lower water contents have a lower freezing temperature but below freezing all samples behave similarly.

The pressure in the unfrozen water phase is known only if the water and ice are in equilibrium. Equilibration was rapid (several minutes) for lamellae in the liquid-crystal phase. When the temperature was changed, the signal intensity initially varied over several minutes and then settled to a value which did not change. Over most of the temperature range, the signal did not change measurably after 10 min. In the range between *ca.*  $-1$  and  $4^{\circ}\text{C}$  the signal continued to change for as long as 60 min. This is the range over which much ice melts for a small temperature change, and it is also the range in which the forces between lamellae are least. Both

effects may be relevant to the slower equilibration. In the results reported, samples were equilibrated for periods between 20 and 90 min (as appropriate) before measurements.

Equilibration was much slower for lamellae in the gel phase. In one experiment, DMPC was first cooled to  $-20^{\circ}\text{C}$  to initiate freezing, left for 30 min, and then warmed to  $(0^{\circ}\text{C})$ , below its phase transition. The NMR spectrum showed a signal with a width of *ca.* 600 Hz which we interpret as unfrozen, motionally anisotropic water in the lamellar phase. There was also a small narrow Lorentzian line with a width of *ca.* 50 Hz. (The spectrum is similar to that for EYL at  $-20^{\circ}\text{C}$ , see Fig. 2.) We interpret the narrow peak as isotropically moving, unfrozen, supercooled water in macroscopic domains. This signal decreased with time, while the broader water signal increased. We attribute this to gradual hydration of the lamellae at the expense of the supercooled water. This process continued over 10 h, with little change in rate over that time. The equilibration time is too long for practical measurements using this technique and for this reason we report no results for lipids in the gel phase.

For temperatures at which the lipids were in the liquid crystal phase, equilibration is rapid and the pressure in the unfrozen water is calculated from eqn. (1). Fig. 3 is a plot of the repulsive force per unit area *vs.* the mole ratio of water to lipid in the lamellar phase. The samples prepared with different total mole ratios all give similar results: at low temperatures, most of the water is frozen and samples with higher mole ratios have a larger volume of ice and the same unfrozen water fraction. In the samples with low mole ratios, all of the ice melted at temperatures below the bulk melting temperature. The error bars in the force represent a possible systematic error in temperature measurement. We have used a worst case of  $0.3^{\circ}\text{C}$ , but we expect that the error is rather less.

Fig. 3 presents the data as a force-hydration relation. The data can be converted to plots of force as a function of separation using eqn. (4), and are shown in Fig. 4. The largest

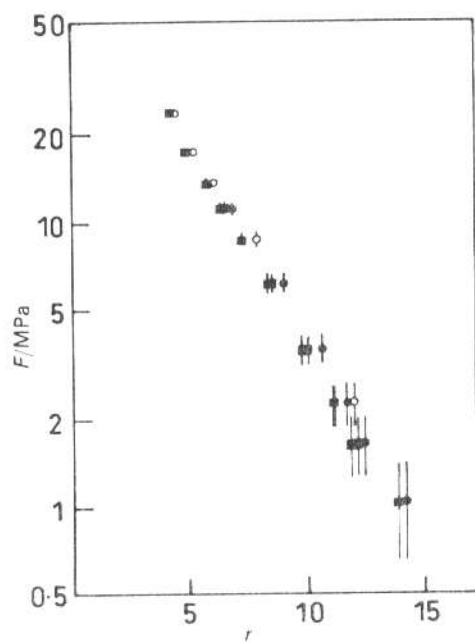


Fig. 3 Interlamellar force per unit area as a function of hydration. The abscissa  $r$  is the mole ratio of unfrozen water to lipid, which is the mole ratio of water to lipid in the lamellar phase. These data were obtained from samples prepared with total mole ratios of (●) 20:1, (■) 37:1 and (○) 50:1. All samples behave similarly below their freezing temperatures.

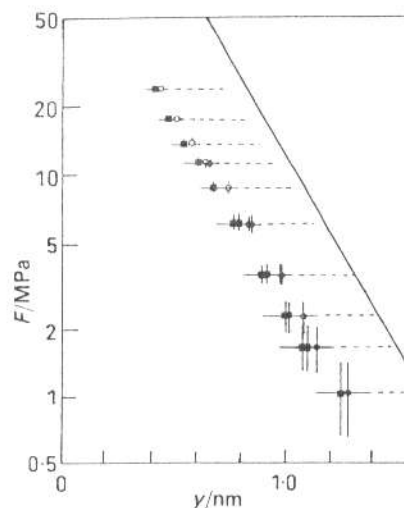


Fig. 4 Interlamellar force per unit area  $F$  *vs.* separation. Symbols as in Fig. 3. The relatively large horizontal error bars are the result of uncertainty about the area per molecule under these conditions.  $0.67 \pm 0.05 \text{ nm}^2$  has been used in the calculation (continuous error bars). The dashed line to the right of each error bar represents the values that would be obtained if one used values in the range 0.62 to  $0.50 \text{ nm}^2$ . The continuous oblique line on the right represents a fit to the data of Lis *et al.*<sup>9</sup> for EYL at room temperature obtained using the osmotic stress technique.

error in calculating the interlamellar spacing  $y$  is the error in the assumed area per molecule. Areas per molecule in lamellar phases have been calculated from X-ray diffraction studies, but there are differences among the values determined by different groups.<sup>1,10,23</sup> Eqn. (4) assumes a constant value for the density of  $\text{D}_2\text{O}$ , taken as the bulk value for these calculations. The area per lipid molecule at full hydration,  $a_0$ , has been taken as  $0.67 \pm 0.05 \text{ nm}^2$  for the calculation. The figure also shows the result of using a larger range of values for  $a_0$ . The values of the area thermal expansivity  $\alpha$  and area elastic modulus  $k_a$  in eqn. (4) introduce an error into  $y$  which is small in comparison with that due to the error in  $a_0$ . For these calculations,  $k_a = 140 \text{ mN m}^{-1}$  (ref. 16), and the effect of thermal expansivity over this range has been neglected.

#### $\text{D}_2\text{O}$ *vs.* $\text{H}_2\text{O}$

The convenience of  $\text{D}_2\text{O}$  in NMR was the reason for its choice in this study. The purpose of the study, however, is to understand interactions in  $\text{H}_2\text{O}$ . Klose *et al.*<sup>24</sup> have measured the sorption isotherms and swelling behaviour of palmitoyl-oleoyl-phosphatidylcholine in  $\text{D}_2\text{O}$  and  $\text{H}_2\text{O}$  and found that, within the limits of the experimental errors, the two systems gave the same swelling curves. This suggests that the results reported here may be compared with those obtained with other methods on  $\text{H}_2\text{O}$ -lipid samples.

#### Comparison with Other Data

Fig. 4 allows comparison of the EYL results of this study with those obtained for the EYL- $\text{H}_2\text{O}$  lamellar phases by Lis *et al.*<sup>9</sup> at temperatures above freezing.† This comparison gives an estimate of the temperature dependence of the repulsive force between membranes. The sign of the temperature

† The results of McIntosh and Simon cited above<sup>10</sup> are not shown because their definition of interlamellar distance is different and this complicates comparison. The definition of separation used by Lis *et al.* is that between the density-weighted surfaces and is thus comparable with the separation used here.

dependence is potentially important to the debate about the origin of these forces. If the forces are mainly due to water structure, then the simplest models predict stronger repulsion at lower temperature. If the forces are mainly due to various modes of thermal motion, the simplest models predict slightly weaker repulsion at lower temperature. Our low-temperature data give repulsions that are smaller than those of Lis *et al.*<sup>9</sup> The slopes of the semi-log plots are similar. In interpreting our data, it should be remembered that for this method, temperature increases with separation. Thus the characteristic length derived from the slope of Fig. 4 should be respectively greater or less than that of an isothermal force law, depending on whether the force increases or decreases with temperature.<sup>4</sup>

#### Comparison with Other Techniques

This technique of measuring force–distance relations was developed primarily for use in the range of temperatures just below freezing, the range over which strong repulsive forces become important in cryobiology. Nevertheless it has several features which may prove to be useful in other applications. The most obvious limitation of the technique is that the experimenter is not free to choose the temperature. This limitation may not be too serious in cases where temperature dependence is slight. A further weakness is that only the quantity of unfrozen water is determined, rather than the separation. This is not a problem if the results are presented as force–hydration relations. Force–separation relations may only be derived for systems in which some geometrical details, such as the interfacial area or the surface: volume ratio of the non-aqueous phase, are known. To a much lesser extent, determination of separation is also a problem in the other force–distance methods: the osmotic stress technique uses X-ray diffraction which determines the repeat spacing much more readily than the interlamellar separation; and the optical interferometry of the SFA determines changes in separation readily, but calculation of absolute separation requires assumptions about the membranes and the surface of mica.

One of the advantages of the technique described here is that the NMR spectrum supplies information about the average orientation of water molecules. This information is potentially of use in explaining the origin of the force in question. Information about the lipids, especially their phase properties, can also be obtained. A further advantage is that it can in principle be applied in cases where long-range order

is absent. Finally there is an appealing elegance in an experiment in which forces and displacements are determined from two measurements of voltage across lengths of wire: a thermocouple and an induction coil respectively.

This research was supported by a grant from the Australian Research Council.

#### References

- 1 R. P. Rand and V. A. Parsegian, *Biochim. Biophys. Acta*, 1989, **988**, 351.
- 2 S. Marčelja, in *Liquides aux Interfaces/Liquids at Interfaces*, ed. J. Charvolin, J. F. Joanny and J. Zinn-Justin, Elsevier, Amsterdam, 1990.
- 3 J. N. Israelachvili and H. Wennerstrom, *Langmuir*, 1990, **6**, 873.
- 4 G. Bryant and J. Wolfe, *Cryoletters*, 1992, **13**, 23.
- 5 J. Wolfe, *Aust. J. Plant Physiol.*, 1987, **14**, 311.
- 6 J. Wolfe and G. Bryant, in *Mechanics of Swelling: from Clays to Living Cells and Tissues*, ed. T. K. Karalis, NATO ASI Series H, 1992, vol. 64, pp. 205–224.
- 7 D. M. LeNeveu, R. P. Rand and V. A. Parsegian, *Nature (London)*, 1976, **259**, 601.
- 8 J. N. Israelachvili, *Faraday Discuss. Chem. Soc.*, 1977, **65**, 22.
- 9 L. J. Lis, M. McAlister, N. Fuller, R. P. Rand and V. A. Parsegian, *Biophys. J.*, 1982, **37**, 657.
- 10 T. J. McIntosh and S. A. Simon, *Biochemistry*, 1986, **25**, 4058.
- 11 R. G. Horn, *Biochim. Biophys. Acta*, 1984, **778**, 224.
- 12 C. Helm, J. N. Israelachvili and P. M. McGuiggan, *Science*, 1989, **246**, 919.
- 13 J. Wolfe, E. Perez, M. Bonnano and J-P. Chapel, *Eur. Biophys. J.*, 1991, **19**, 275.
- 14 *CRC Handbook of Chemistry and Physics*, ed. R. C. Weast, CRC Press, Boca Raton, FL, 1984.
- 15 *Chemical Index*, ed. S. Budavari, Merck, Rahway, NJ, 1987.
- 16 R. Kwok and E. Evans, *Biophys. J.*, 1981, **35**, 637.
- 17 J. H. Davis, *Biochim. Biophys. Acta*, 1983, **737**, 117.
- 18 T. J. James, *Nuclear Magnetic Resonance in Biochemistry — Principles and Applications*, Academic Press, New York, 1975.
- 19 K. Beyer, *J. Colloid Interface Sci.*, 1982, **86**, 73.
- 20 N. J. Salisbury, A. Darke and D. Chapman, *Chem. Phys. Lipids*, 1972, **8**, 142.
- 21 J. M. Pope, L. Walker, B. A. Cornell and G. W. Francis, *Biophys. J.*, 1981, **35**, 509.
- 22 G. Bryant, J. M. Pope and J. Wolfe, *Eur. Biophys. J.*, 1992, **21**, 363.
- 23 D. M. Small, *J. Lipid Res.*, 1967, **8**, 551.
- 24 G. Klöse, B. König and F. Paltauf, *Chem. Phys. Lipids*, 1992, **61**, 265.

Paper 3/00758H; Received 8th February, 1993